NASA TM 75333

OPTICAL MEASUREMENT METHODS IN THERMOGASDYNAMICS

K. Stursberg, K. Erhardt, W. Krahr,
and M. Becker

NATIONAL AERONAUTICS AND SPACE ADMINISTRATION
WASHINGTON, D.C./ 20546   OCTOBER 1978

1. Report No. NASA TM-75333 .	2. Government Accession No.	3. Recipient's Catalog No.
4. Title and Subtitle OPTICAL MEASUREMENT METHODS IN THERMOGAS-DYNAMICS		5. Report Date October 1978
		6. Performing Organization Code
7. Author(s) K. Stursberg, K. Erhardt, W. Krahr, and M. Becker		8. Performing Organization Report No
		10. Work Unit No
9. Performing Organization Name and Address .SCITRAN Box 5456 Santa Barbara, CA 93108		11. Contract or Grant No NASW-3198
		13. Type of Report and Period Covered Translation
12. Sponsoring Agency Name and Address National Aeronautics and Space Administration Washington, D.C. 20546		14. Sponsoring Agency Code

16 Abstract

A review is presented of a number of optical methods of flow measurements. Consideration is given to such spectroscopic methods as emission and absorption techniques, electron beam-stimulated fluorescence, and light scattering ——Rayleigh, Raman and Mie —— methods. The following visualization methods are also discussed: shadow photography, schlieren photography, interferometry, holographic interferometry, laser anemometry, particle holography, and electron-excitation imaging. A large bibliography is presented and the work is copiously illustrated with figures and photographs. B.J.

17. Key Words (Selected by Author(s))		18. Distribution Statement Unclassified - Unlimited	
19. Security Classif. (of this report) Unclassified	20. Security Classif. (of this page) Unclassified	21. No. of Pages 62	22.

NASA-HQ

Contents:

1. Introduction

In flow mechanics, particularly in thermogasdynamics, the trend from probe measuring methods to optical measuring methods is becoming increasingly apparent and compelling. In spite of important results in the theoretical sector, the characterization of flow fields, energy and material exchange processes and chemical reactions in general is possible only if information obtained by measuring techniques is available from the partial areas of the range of investigation. Such information relates to the composition of the medium to be investigated, the distribution of pressure, density, temperature and velocity, material properties, reaction times and several other values.

The problems arising from these circumstances with respect to the technology of measuring are fundamentally always the same. They are:

1) What particles are present in the volume being investigated (molecules, atoms, ions, electrons)?

2) How many particles of each type are present in unit space (partial densities, concentrations)?

3) What are the disordered (thermal) velocities of these particles (temperature)?

4) What is the ordered (macroscopic) velocity of the particles (velocity and direction of flow)?

In special cases, the following additional questions arise:

5) Are the discrete energy levels of the molecules (rotation, vibration, electronic stimulation) occupied in accordance with the Boltzmann statistic by the uniform thermodynamic temperature?

6) Do the distribution of the dissociation products obey the mass

effect law and the distribution of the ionization products the Saha equation?

7) How do the parameters of state vary with time and space?

The gradients of the parameters of state, in addition to the macroscopic flow velocity, are responsible for the transport of mass, heat and impulses. In the last analysis, these exchange parameters characterize any thermogasdynamic process. Diffusion, thermal conductivity and friction may be represented formally by the same relationship:

ORIGINAL PAGE IS
OF POOR QUALITY

$\ddot{J}$ =	- C	grad ϕ
Flow parameter	Material property	Driving force
mass flow	(diffusion coefficient,	(concentration gradient,
Heat flow	thermal conductivity,	temperature gradient,
Impulse flow	viscosity)	velocity gradient)

Material constants may be calculated by the kinetic gas theory or it may be determined experimentally. Their dependence on the type of molecule, temperature and pressure may be considered either as adequately known or as a subject for research by other specialties. Flow mechanics therefore require the determination of the composition and the concentration, temperature and velocity profiles in order to create necessary experimental conditions for the description and calculation of flow phenomena and the coupled exchange processes.
Let us mention for the sake of completeness that in numerous cases the exchange of energy by radiation must also be taken into account; this exchange is also defined if the state parameters cited are known.

The necessary measured values must be determined free of interference as much as possible, i.e. the method of measurement must not cause any change in the value to be measured, except if the changes are accurately defined and are controllable. Further, the measurements should be performed locally and with the best possible time resolution. In addition, nearly every point in the flow field should be accessible, regardless of the geometry of the boundaries and the thermal condition of the flow.

In principle, all of these requirements may be satisfied if light beams are use as alternatives to material probes. Even though substantial difficulties exist in part in the conduct of such measurements, the problems in general are resolvable, as indicated by the optical methods practiced at this time.

2. Interaction Between Light and Material

In order to characterize the numerous optical measuring methods in existance, it is advisable to briefly discuss the interaction between light and material. It is known that all atoms and molecules are capable of storing discrete energy contributions. The motion of the electrons around the nuclei of the atoms, and the rotational and vibrational movements of the nuclei around the center of gravity of the molecules may be considered as storage mechanisms. All movements of material particles are characterized by the mass moved, the velocity and the path covered. The product of these values (m.v,l) is designated the action.
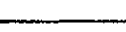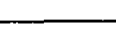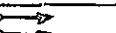
Planck has shown that in the internal atomic range the cation cannot assume any arbitrary value, but that there exists a smallest unit which is not exceeded downward and which defines the packets of energy transferred in all processes of exchange, the so-called energy quanta. This concept assumes that

only discrete states of energy may exist and only discrete states of energy may
be exchanged. The graphical representation of these facts yields the so-called
energy level diagram, a plotting of possible energy levels as a function of
the distance from the nuclei of the molecules.

Something similar is true for light. Light may be imgained as concentrated and
localized in small particles, the so-called photons, which propagate linearly
at the speed of light. The energy of such a photon is always a multiple of
the action quantum ($h \cdot \bar{\nu}$); changes in its energy are also quantized ($h \cdot \overline{\Delta \nu}$).
Because of coupling by means of the action quantum h, light and material inter-
act when they coincide. In the process, the following energy exchange processes
may take place:

TABLE

Before	After	Designation	ΔE
〜〜→ ○	⊛	Absorption	$h\nu$
⊛	○ 〜〜	Spontaneous emission	$h\nu$
〜〜→ ⊕	○ 〜〜 〜〜→	Stimulated emission	$h\nu$
〜〜→ ○	⊛ 〜→	Raman scatter (Stokes)	$h\Lambda\nu$
〜〜→ ⊕	○ 〜〜→	Raman scatter (Anti Stokes)	$h\text{B}\nu$
〜〜→ ○	○ 〜〜→	Rayleigh scatter	0
〜〜→ •	•→ 〜〜→	Compton effect (bound electron)	$h.\Lambda\nu$
〜〜→ •	• 〜〜→	Thomson scatter (free electron)	0
•→ ○	⊕ •→ •→ 〜〜→	Electron beam fluorescence	$h\nu+E$

Photon,: Electron; ○ Atom or molecule in the ground state
〜〜→ • ⊛ Atom or molecule in the excited state

During absorption and emission, the electrons undergo energetic changes in their
external shells (optical electrons); the energy quantities exchanged in the process are relatively large compared to those exchanged in scattering. In the case of Raman scattering, the rotation and vibration levels are altered, without a change in the energy of the electrons. In Rayleigh and Thomson scattering there is no exchange of energy at all, photons are merely deflected in their direction.

It is possible that an absorption process is followed immediately (in about 10^{-8} sec) by an emission process. This phenomenon is designated fluorescence. If the period of time between absorption and emission is large, the phenomenon is called phosphorescence. The energy absorption in fluoresecence is not restricted to the capture of photons, it may also be the result of a collision interaction between two atoms or between an atom and a free electron. Let us include the latter interaction in the discussion of "massless probes", because of the small masses involved.

Another mode of defining light consists of a description of macroscopic phenomena connected with the propagation of light. The coarsest variation of such a description consists of defining light as beams of bundles of light. For everyday use and the field of geometrical optics such a description is entirely justified and adequate. The situation becomes critical only when certain phemonena which may be observed at the boundaries of bundles of light and in their superposition, such diffraction, refraction, interference, are to be explained physically. To interprete such phenomena, one must proceed to the second kind of the description of light, i.e. to the wave theory of light.

This theory states that light is an electromagnetic wave phenomenon existing

within a certain wave range. The basis of a description of wave propagation is the Huygens principle, which states:

The propagation of a wave takes place by that from every point of an existing wave surface an new elemental, spherical wave goes forward. The envelope of the elemental waves -- with all points of the old wave surface as centers -- yields the surface of the wave at a later point in time.

With this principle, which is valid for all types of wave propagation, the laws of reflection, refraction diffraction and interference may be derived directly. Even the Doppler effect, which appears as a shift in frequency between the emitter of the wave and the receiver and the phneomenon of polarization, the vibration of light waves in certain planes, may be readily understood in view of the wave character of light.

Wave optics forms the theoretical basis of the following measuring methods:

Method	Physical effect	Measured value
Shadow and Schlieren method	Deflection of light rays by grad ϕ	$n[x, y] \rightarrow$ ρ, T, c
Interferometry (conventional and holographic)	Phase position changes through grad ϕ	$n[x, y(z)] \rightarrow$ ρ, T
Anemometry	Mie scattering	$v[x, y (z)]$
Particle field holography	Diffraction	$N (+) = f(x, y, z)$ $v(x, y, z)$

The dual nature of light, which is manifested in its corpuscular and its wave mechanical behavior, should not be understood as meaning that light has two phenomenological forms or that it reacts in two ways in its interactions

with matter. The concept that light -- depending on the conditions of obser-
vation and the mode of measurement -- behaves as particulate matter or as a
succession of waves, without actually being one or the other, is more realistic.
Advanced quantum mechanics provides the mathematical apparatus to describe all
interactions between light and matter both in keeping with the particle image
and the wave concept completely and uniformly. In the process, however, the
pictorial content of the model concepts is largely lost. For actual practice
it is therefore convenient to remain on the ground of classical physics.and to
use the dualistic mode of imaging. Let us therefore restrict ourselves to
these imaginative modes of viewing light and with coarse simplification accept
the assumption that the microanalysis of flows, i.e. the identification of mo-
lecules by type and state of energy is described by the particle model and
macroanalysis, i.e. the visualization of the flow, by the wave model.
The result is the division of optical measuring methods into <u>spectroscopic</u>
<u>methods</u> which treat of energy exchange processes between light and matter
and therefore must be "energy selective" and the <u>imaging methods</u>, which are
based on the wave like propagation of light in matter.

3. <u>Spectroscopic Methods</u>

3.1 <u>Absorption and Emission</u>

The property of atomic and molecular systems to take up quanta of energy or
emit them has been utilized for a long period of time in emission and absorp-
tion spectroscopy.
While in absorption the volume to be examined is illuminated by a suitable
source of light and conclusions are drawn with respect to density and tempe-
rature from the frequencies absorbed, emission spectroscopy uses the self-
luminiscence of of a heated gas in the analysis.

This signifies that emission spectroscopy is possible at sufficiently high temperatures only, at which excited atoms or molecules are present in adequate numbers.

Both methods have in common the fact that the information obtained through them is integrated over the entire layer of gas investigated. Although it is possible in many cases (e.g. in case of rotational symmetry) to determine local temperatures or densities by means of mathematical inversion, the application of the methods to processes with strong gradients is very limited.

For this reason, absorption and emission spectroscopy shall not be discussed here in more detail; an extensive literature is available /1, 2, 3, 4/.

3.2 Electron Beam Fluorescence

In our own DFVLR experience the method of electron beam induced fluorescence is being used.to obtain spatially well resolved information concerning parameters of state. This provides means to measure the densities and temperatures of the gas directly. Its functioning is based on the interaction of electrons high in energy with the molecules of the gas flow. Several effects occur in the process:

. scattering (elastic collision)

. braking in the Coulomb field of the nucleus with the emission of x-rays .

. stimulation of rotational and vibrational transitions in the molecule and simultaneously

. stimulation of electron transitions with subsequent emission of electromagnetic radiation

. dissociation and ionization of the molecule.

The macroscopic consequence of these processes is a strong fluorescence,

an intensive luminescence of the gas in the area of the electron beam. Spectros-

copic analysis of this light emission exhibits for example in the case of a

flow of nitrogen the characteristic molecule bands of nitrogen.

The distribution of the rotational and vibrational structure of the molecular

bands depends on the occupation of the corresponding energy levels in the mo-

lecule and thus on the temperature.

The total intensity of fluorescence is a function of gas density.

The strength and the weakness of the electron beam method lies in its restric-

tion to gas densities of $\leq 10^{-1}$ of standard density. At higher densities

the electron beam is rapidly expanded by scattering and intermolecular col-

lision processes (quenching) interferes with fluorescence to the extent that

evaluation becomes impossible. On the other hand, the electron beam method

operates within a range which is accessible to laser light scattering methods,

among others because of the very small interaction cross sections, only

with difficulty and substantial cost. The laser and electron beam methods thus

supplement each other in an ideal manner.

The low gas density, which is a precondition of the use of electron beam ana-

lysis, on the one hand excludes the investigation of many flow processes

in the field of aeronautics, but on the other hand makes possible the exami-

nation of numerous thermodynamic processes observable only at such low gas den-

sities. Gas dilution is used as a parameter in scale enlargement in the ana-

lysis of flow and reaction processes.

The functioning of the electron beam technique may be explained by the follow-

ing discussion:

The electron beam is passed through the volume of gas to be investigated

with an acceleration potential of approx. 20 kV and an intensity of approx.

1 mA. During the collision of electrons with gas particles, they are raised from their initial electronic ground state of E_0 to an excited state of E_1. describes this process with the applicable energy levels in the ground state, in the ionized ground state and in the ionized excited state. From the E_1 state the gas particles return to a stable electronic state E_2, accompanied by the release of photons.

The three way division of the total energy of the molecule in the electron excitation energy, the vibrational and the rotational energy corresponds to the three part structure of band spectra. The latter consist of a number of bands and each band of a series of individual lines.

The greatest change in the total energy of a molecule occurs during electron transition. The magnitude of this transition thus determines the position of a band system in the total spectrum. All of the bands of a system belong to the same electron transition. Their position in the system is determined by the difference in vibration energy in the initial and the final state. Finally, the different lines of a band belong to different rotation quantum jumps. The vibration temperature may be derived from the intensity ratio of two bands. The intensity distribution within the rotational structure of a band permits conclusions concerning the rotational temperature.

The transitions and emissions of interest for diagnostuc purposes, are characterized in a model of the diatomic nitrogen molecule in Fig. 2. This representation involves the first negative system with an excitation energy of 19 eV and the second positive system with an excitation energy of 11 eV. The higher energy level (ionizied) yields the information desired concerning the vibrational and rotational structure; the lower energy level (excited) provides indications concerning the concentrations of primary and secondary electrons /5/.

The fluorescent light emitted is collected by means of an optical apparatus adapted to the measuring problem from a small measuring volume (disc-like section of the column induced by the electron beam) and analyzed spectroscopically with a monochromator. (Fig. 3).

The vibration temperature is given by the ratio of the peak intensities of two bands, e.g.

$$T_v = f \ (I_{0,1}/I_{1,2})$$

If it is permissible to assume a thermodynamical equilibrium between the rotational and vibrational temperatures in the investigation of gaseous states, the determination of the rotational temperature at a low temperature level is simple and characteristic for the state of the gas. Fig. 4 from /6/ shows the variation of spectral intensity in the N_2^+ (0,0) band near 391 nm for a temperature of 300°K. This indicates that the rotational structure consists of two wings, the well resolved R branch and the P branch, which is not resolved because of selfoverlapping.

The rotational temperature may be determined by measuring the maximum intensities in the R branch and the maximum intensity in the P branch:

$$T_{Rot} = f \ (I_{P, \ max} \ / \ I_{R,K, \ max}).$$

Here, $P \rightarrow \Delta K = -1$ and $R \rightarrow \Delta K = +1$.

With rising temperatures the number of lines visible in the spectrum increases. Additionally, lines of the P branch appear; these are in the wave range of the R branch. The branches are beginning to overlap and the usual method (Boltzmann plot) to determine the temperature can no longer be used.

For this reason, Schweiger /6/ developed a method which compares such a spectrum with a calculated spectrum. In the synthetic spectrum the maximum intensity of the P branch and the intensities of the R branch were related to each other for the measured K values (Fig. 5 of /6/). These characteristics depend on the rotation temperature; they yield temperatures with acceptable

accuracy to approx. 4000°K.

Density is determined by means of the total intensity or the maximum intensity of the P branch. In the case of several components the composition of the gas may be determined by means of the intensity distribution of the entire spectrum established.

The following discussion is to serve as a characterization of the applications of electron beam analysis. Fig. 6 /7/ provides a view of the experimental arrangement of a measurement related to collision-collision interference. A model of a planar plate was placed in the measuring chamber, together with with a transversely set cylinder (10 mm diameter) to produce an oblique densifying impact. The power of resolution of the electron beam probe was approx. 1 mm^2.

The rotation temperatures shown in Fig. 7 /7/ display the collision interaction. For comparison, the temperatures developing without the presence of the other collision are also plotted. The transition from the cylinder impact (high Y values) to the plate impact range with a clear boundary temperature maximum is readily discernible. Such an interference phenomenon would be determined with a material probe with severe measuring errors only .

Fig. 8 /8/ visualizes the energy distribution in a nonequilibrium for in front of a spherical model.

The flow, coming from the undisturbed free flow field ($x/\lambda_\infty >> 1$) impacts the stagnation point of the sphere model at x = 0; λ_∞ is the average length of free path of the flow of air. The area between x/λ_∞ = 0.5 and 1 is the impact zone in which the rotation temperature rises strongly as the result of the absorption of kinetic energy. Further variations of the temperature to the stagnation point is characterized by the transfer of heat to the model.

Vibration energy was on a high level in the oncoming flow already so that in connection with a very long relaxation time only a monotonic transition to the model temperature could be determined.

3.3 Light Scattering Methods

During the passage of light through matter intensity undergoes attenuation not only because of absorption, but also -- even though a much weaker one -- because light scattering. In a simplified manner, scattered light may be defined as the portion deflected from the direction of propagation during the passage of light through matter; it is being scattered in all directions. An impressive proof of the scattering of light is the blue color of the sky. Would there be no light scattering, the sky in daytime would be absolutely black except in the direction of the sun (neglecting the stars). Another well known light scattering phenomenon is the beam of sun rays shining into a dark room, which is clearly visible when viewed from the side. The fact that /13 a beam of light may be viewed from the side is the result of the interaction between light and matter. This interaction offers interesting possibilities concerning information relating to the matter through which the light passes. Because a beam of light may be bundled very finely and because it is possible to scan the beam laterally from point to point by means of a suitable recording optical device, a local measuring method can be developed from the phenomenon of light scattering.

Depending on the type of the scattering particles, the following theories and methods are distinguished:

Scattering particle	Theory of	Method	Result
Free electrons	Thomson	Thomson scattering	n_e, T_e v_D
Atoms and spherically symmetrical molecules	Rayleigh	Rayleigh scattering	$[T, v]$
Molecules	Raman	Raman scattering	ρ, T
Aerosols, dust particles	Mie	Mie scattering	$N(r)$

The extreme situation of plasmas shall be disregarded, because it plays a subordinate role in flow mechanics in comparison with non-ionized flows, i.e. Thomson scattering will not be discussed in detail. Let us merely mention that the method can be used to determine the concentration and velocity distribution of free electrons, from which in turn conclusions may be drawn concerning temperature distributions and drift velocities. The Thomson scattered light is shifted in frequency to the Doppler shift.

A more interesting field consists of molecular scattering, such as is manifested for example by the blue of the sky. If one views the interaction between photons and molecules as collision processes, then it becomes necessary to distinguish between elastic and inelastic collisions. An elastic collision process exists when a photon is merely deflected away from its original direction, without a change in energy. The scattered photon thus has the same energy as the exciting light. Such a scattered light -- without a shift in frequency -- is designated a Rayleigh light. When the collision process is inelastic, meaning that energy is being exchanged between the molecule and the photon, then the scattered photon changes its frequency and frequency-shifted light is generated, the so-called Raman light.

3.3.1 Rayleigh Scattering

Rayleigh scattering is well suited for local density determinations, if the gas consists of a single component. The measuring method is diagrammed in Fig. 9.

By determining in addition to the peak value, the exact position and the shape of the Rayleigh lines, then with consideration of the monochromator effect the frequency shift with respect to λ_∞ and the half-width of the line may be ascertained. Any shift in frequency is to be attributed to the Doppler effect resulting from the directional flow velocity. The difference between the measured line width and the natural line width is a measure of the thermal Doppler effect. Therefore, from the Doppler broadening the temperature T and from the Doppler shift the directional velocity v may be determined. It is true, however, that the Fabry-Perot technique required is costly. And because certain other phenomena make it difficult to determine the Rayleigh line exactly, if possible, other methods should be used for the determination of T and v.

If the volume to be examined contains several species of gases, possibly of unknown identity and concentration, then the evaluation of the Rayleigh signal is practically no longer feasible. Scattering cross sections differ with the components, molecular weights yield different thermal velocities and thus different line profiles, the relative signal proportions of the individual components are undetermined, i.e. the evaluation of the measuring signal is difficult.

The advantage of Rayleigh scattering is in its relatively broad scattering cross section and high signal level, respectively, yielding a good signal to noise ratio. This measuring method thus appears to be particularly suitable for the investigation of nonstationary processes in flows of known composition.

For example, turbulent fluctuations of a velocity that is not excessive, may

be resolved with respect to time by means of a high capacity continuous wave

laser /9/. The importance of Rayleigh scattering resides in this area.

3.3.2 Raman Scattering /10-20/

If the collision process between photons and molecules is inelastic, the pho-

ton in addition to the change in direction undergoes a change in energy and

frequency, respectively:

$$h\nu_0 \rightarrow h\cdot(\nu_0 - \Delta\nu)$$

This change in frequency is expressed by the spectrum of the scattered light

by the appearance of a plurality of lines besides the Rayleigh line; the genera-

tion of these lines shall be explained with the aid of **Fig. 10.**

The law of the preservation of energy states that the change in the energy of   /15/

the photon is equal to the change in the energy of the molecule:

$$h \cdot \Delta\nu = E_1 - E_0 ,$$

where E_0 is the energy of the molecule before and E_1 its energy after the col-

lision.

The diagram shows schematically the rotational energy levels indicated by the

quantum number J and the vibrational energy levels designated by the quantum

number v. Let a photon enter into interaction with a molecule which for example

is in the ground state v = 0, J = 0, the two will then form a single unit for

a very short period of time, the energy of which is shown by the broken line

(virtual or intermediate level). This amount of energy does not represent a

stable energy level of the molecule. Consequently, the unit will emit energy

in order to reestablish its molecular state of equilibrium.

When by energy emission the initial level has again been attained ($\Delta v = 0$),

Rayleigh light scattering is generated, which has been discussed before: If

the molecule assumes a somewhat higher state of energy ($\Delta v > 0$), the so-called

Stokes Rama scattered light is obtained which is shifted toward longer waves

with respect to λ_o. If the molecule loses energy in the interaction ($\Delta v < 0$)

then anti-Stokes Raman scattered light with shorter wave lengths is generated.

This, however, is possible only when the energy of the molecule had been above

the ground state prior to the collision.

When the molecular energy jog takes place between levels of rotation, the pheno-

menon is called the rotational Rama effect. Correspondingly, the transition

between the vibrational levels is designated the vibrational Rama effect. The

frequency shift Δv is the Raman shift.

In principle, there is no restriction in relation to the energy level involved.

The transitions may take place between all vibrational levels and all rotational

levels and combined rotation-vibration processes are also possible. There are,

however, restrictions with respect to the magnitude of the jump in energy,

these are defined by selection rules

$$\Delta J = 0; \pm 2 \quad ; \quad \Delta v = 0; \pm 1$$

An energy level scheme belongs to each type of molecules; the scheme is not in-

terchangeable. This signifies that the differences between the levels and thus

the Raman shifts are specific to molecules. If monochromatic light is passed

into the sample and the scattered light generated is diffracted with respect

to frequency, the position of the spectral lines relative to the incident

wave length provides a direct indication of the types of molecules contained

/16

in the sample. The only assumption made is that the effects of overlapping

remain within limits and that the individual molecular spectra be recognizable.

Let us cite the scattered light spectrum of air as an example (Fig. 11).

In the case of moderate spectral resolution it is not possible to decide what

components are contained in what concentrations in the sample. Only vibrational spectra indicate by means of their differential wave lengths the types of molecules involved. This unambiguous correlation of molecular types with the Raman shift is the basis for the identification of the components of the gas. Because there is a linear relationship between the number of molecules in the volume investigated and the intensity of scatter radiation, concentrations may be determined directly from the relative intensities.

With a higher resolution of the spectra, the fine structure of the rotation wings becomes recognizable. In **Fig. 12** the rotational Raman spectrum of the air measured at room temperature is given. Although the spectrum appears to be somewhat irregular, it is possible to correlate each line unambiguously a certain quantum jump. Even though the oxygen and nitrogen lines coincide at some points, the overlap is purely additive so that the significance of the lines is not lost.

The constant change in intensity is the result of the thermal occupation of the energy levels. According to Boltzmann statistics, the number of molecules in the J rotational state is:

$$N_J = \frac{N}{Q_{Rot}} \; g_J \cdot (2J + 1) \cdot e^{E_J/kT}$$

N_J = number of molecules at the J rotational level (per cm^3)

N = total number of molecules (per cm^3)

Q_{rot} = sum of state per level of rotation

q_J = statistical weight of nuclear spin

$(2J + 1)$ = degree of degeneration of the level of rotation

E_J = energy of the level of rotation $J = f(J)$

K = Boltzmann constant

T = absolute temperature

J = rotational quantum number

In the case of pure gases the term $(2J + 1) \cdot e^{E_J/kT}$ determines the configuration of the envelope curve resulting from the connection of the intensity peaks, while the factor q_J causes the explicit intensity fluctuations under the envelope curve. To demonstrate this, Fig. 13 presents the rotational Rama spectrum of pure nitrogen.

Because the shape of the envelope curve is determined among others by the Boltzmann factor $e^{E_J/kT}$ the temperature may be determined directly from the slope of the straight line obtained by the logarithmic plotting of the peak intensity over the quantum number J. This temperature is designated the rotational temperature, because it determines the distribution of molecules over the rotational level. In the case of thermodynamic equilibrium, T_{Rot} is identical with the translation and the vibration temperatures.

In principle it is sufficient to relate only two line intensities to each other to obtain T_{Rot}. To improve the accuracy, however, it is advisable to evaluate the entire spectrum. The accuracy attainable may be given as better than 5%; with more extensive equipment and favorable experimental conditions, accuracies to 1% may be obtained.

If the temperature is determined by the comparision of relative intensities, then by evaluating the absolute intensity of the lines the total number of molecules in the volume under investigation may also be determined.

The temperature may be determined from the vibrational lines in a manner similar to the determination from the rotational lines. Because of the favorable spectral position of the vibrational lines, the vibration temperature is often simpler in many practical cases, because the spectral lines desired may be selected by means of interference filters, which renders the expensive monochromator operation unnecessary. Such an arrangement is shown in Fig. 14.

20

The temperature profile of an open butane flame was measured with this apparatus; the result is shown in Fig. 15. Deviations from thermocouple measurements are slight, they may be attributed primarily to fluctuations in the unstabilized flame.

Vibrations temperatures may be determined with particular ease when temperature levels are high ($>$ 1000°K); then the excited vibrational levels are adequately occupied so that in addition to the ground vibration transition other vibrational transitions also provide measurable intensities. At lower temperatures ($<$ 500°K) evaluation of the rotation spectrum is more favorable.

Molecular scattered radiation is characterized by very small action cross sections, /18 i.e. by very weak intensities. For this reason, this effect may be used for measuring technical purposes only if very strong monochromatic light sources (e.g. lasers) and highly sensitive detectors and electronic signal processing units are employed. Scattered light measuring techniques are thus expensive and somewhat diffcult in handling. On the other hand, the technique is tempting, because all of the information necessary for the definition of thermogasdynamic processes is produced locally and free of interference.

In order to circumvent the difficulties arising from the small scatter cross sections, the "coherent anti-Stokes Raman scatter" (CARS) was introduced, which at similar Laser capacities is much more effective than spontaneous Raman scatter. It is reported that the method increases the intensity of scattered light by 6 orders of magnitude or more /21-25/.

3.3.3 Mie Scatter

A beam of light observable from one side becomes visible because of the so-called Mie scatter. Mie scatter is the process in which light is scattered by

dust particles, smoke or fog, i.e. particles generally present in gaseous media and entrained in flow because of their smallness. A Mie scattering particle with a diameter of 1 μm produces about 10^{20} times as much scattered light as a molecule, individual Mie particles may thus be observed directly. This fact is utilized in laser-Doppler anemoetry, in which conclusions are drawn from the scattered light of individual particles concerning the velocity of the carrier medium. In every day life suspended in air (aerosols) play a large role, because they are capable of affecting the quality of air, decisively influence the weather and determine visibility ranges. They also are involved in combustion processes. The effectiveness of a combustion chamber depends largely on the particle size and distribution generated during the atomization of fuel and on the formation of soot particles.

The theory of light scattering on spherical particles with diameters of the order of magnitude of the length of light waves was formulated as early as 1908 by Mie /26/. It follows from this theory concerning volume scattering, when particles of different sizes are involved in the scattering process, when i.e. in addition to the total number the size distribution N(r) of the particles must also be considered that /27/:

$$I(\phi) = E_0 \cdot \frac{\lambda^2}{8 \pi^2 R^2} \cdot \int_{r_1}^{r_2} \left[i_1(\phi,\alpha,n) + i_2(\phi,\alpha,n) \right] N(r)dr$$

$I(\phi)$	= scatter light intensity in the ϕ direction
E_0	= irradiation intensity at the particle location
λ	= wave length of irradiation
R	= particle to receiver distance
i_1, i_2	= functions given by Mie
α	= size parameter = $2 \pi r/\lambda$
n	= refraction index of particles
N(r)	= size distribution of particles
r_1, r_2	= boundary radii of particle distribution

22

It is seen that the scattered light contains information containing the type

of particle (refraction index n), particle size ($\boxed{\alpha}$ and r) and size distribu-

tion. If all of these data are unknown, it would be extremely difficult to ex-

tract them from the scat$\boxed{\text{tered}}$ light signals. If, however, the particle size

distribution can be determined by other measuring methods (for example hologra-

phically or by means of laser-Doppler anemometry), there is hope of $\boxed{\text{being able}}$

to identify the type of particle$\boxed{\text{. Mie scattering has been mentioned here to}}$

present a closed discussion of light scattering methods. It belongs more to

the imaging methods than to the spectroscopic procedures. The intensity equa-

tion given has been obtained not from the corpuscular, but from the wave me-

chanical mode of viewing light. Details of application may be found in /10/.

4. Imaging Methods

The imaging methods to be discussed here are essentially optical methods which

visualize density gradients in $\boxed{\text{transparent flows}}$ and make possible the study

of particle fields and movements, without causing interference through an ex-

change of energy with the material studied. In contrast to spectroscopic

methods, here it is not the spectral intensity distribution of the light re-

corded but the spatial, macroscopic intensity distribution, including variations

in time. In other words, the frequency selection by means of a monochromator

is replaced by various methods to record bright-dark fluctuations.

Density gradients in gases cause changes in the refraction index; the relation- $\boxed{/20}$

ship between density and the refraction index is described by the Lorenz-Lo-

renthz law

$$N(\lambda) = \frac{n(\lambda)^2 - 1}{n(\lambda)^2 + 2} \cdot \frac{M}{o}$$

and for n = 1 by the Gladstone-Dale law:

$$N(\lambda) = \frac{2}{3} [n(\lambda) - 1] \cdot \frac{M}{o} \qquad ,$$

Here

$[\mathfrak{N}(\lambda)]$ = mole refraction = $[(4\pi/3)]\cdot L\cdot$ Losschmidt number

$[\alpha]$ = polarizability constant = $f([\lambda])$

$n([\lambda])$ = index of refraction

M = molecular $[weight]$

$[\rho]$ = density

$M/[\rho]$ = mole volume = $RT/[\rho]$

For a given wave length therefore approximately $n - 1 = k\cdot[\rho]$.

The visualization of changes in the index of refraction occurs either by means of the recording of the deflection of light rays from the direction of propagation (shadow and schlieren technique) or by recording the changed phase position of the waves of light (inferometric methods).

If not homogeneous media, the interaction with incident light is being investigated, are involved, but discrete particles, other mechanisms of visualization are used. The previously mentioned Mie scatter is used to determine the velocities of discrete particles by means of light scattering produced by their passing through light marks. (Laser-Doppler anemometry and laser two foci method). Particle fields are investigated (size and number) with the aid of refraction phenomena, wherein holographic storage and reproduction techniques are utilized.(particle field holography). At low densities, where changes in the refractory index have no measurable effect on the passage of light ($n = 1 = K\cdot[\rho]$), molecules are excited to luminescence so that conclusions concerning the density of the gas may be drawn from the local intensity, (gas discharge methods and electron beam stimulation).

In the following some brief explanations of the methods mentioned will be pre-
sented. Holographic inferometry, which is considered important, will be dis-

24

cussed in somewhat more detail.

4.1 Shadow Technique

In the shadow technique, the transparent medium to be investigated is irradiated by light and the exiting light collected on a screen. As the result of differential light refraction in media of varying density, the brightness distribution on the screen differs from that obtained with homogeneous density distribution. In principle, any type of light source may be used for the irradiation. However, interpretation is simpler when parallel monochromatic light is used. Designating the homogeneous reference state by the index 0, results is:

$$n - 1 = (n_0 - 1) \frac{\rho}{\rho_0}$$

For fluctuations in illumination on the image screen element, dxdy, which through beam deflection $(\alpha x, \alpha y)$ changes into

$$1 \cdot dxdy \cdot \frac{\partial \alpha x}{\partial x} + \frac{\partial \alpha y}{\partial y} \quad ,$$

followed by

finally

$$\alpha x = \frac{1}{n_0} \int_O^L \frac{\partial n}{\partial x} \, dz \text{ and } \alpha y = \frac{1}{n_0} \int_O^L \frac{\partial n}{\partial y}$$

$$\frac{\Delta I}{I} = - \frac{1}{n_0} \int_O^L \left(\frac{\partial^2 n}{\partial x^2} + \frac{\partial^2 n}{\partial y^2} \right) dz$$

where

l = distance between the object and the screen

L = length of the object irradiated.

The fluctuation of the illumination is thus proportional to the second derivative of the inder' of refraction with respect to spatial coordinates. Additional details, examples of applications and references may be found in /28/.

4.2 Schlieren Technique

The schlieren technique closely ressembles the shadow method. As in the focussed shadow method, the parallel beam which penetrates the volume to be investigated, is focussed by means of a concave mirror or lens and imaged through a second lens on the image screen. In contrast to the shadow method, however, a "schlieren diaphragm" is introduced in the focus, which covers one half of the image beam. If there are no density gradients in the volume to be investigated, the image is uniformly attenuated on the screen without altering the content of the image. If, on the other hand, density gradients are present, the schieren diaphragm passes fewer or more ligh rays, depending on the orientation of the gradient. Refraction away from the schlieren edge leads to lightening, refraction onto the schlieren edge results in darkening. Because the laws of reproduction are not affected by the schlieren edge (only the intensity changes) the lighter-darker phenomena appear in locations which are co-ordinated with the position of the density gradient in the experimental volume, with respect to imaging.

The schlieren diaphragm may consist of circular diaphragms, straight edges, color strip filters and color flat filters. The different schlieren diaphragms are developed in order to unamiguously define the deflections of the light beam with respect to magnitude and direction. The color effect facilitates the identification of intensity differences by producing mixed colors, while the shape of the edge indicates the direction of the density gradient. The schlieren technique is not restricted to parallel light in the range investigated; convergent and divergent light also produce very good schlieren images, particularly since in general only qualitative information is required. Under certain conditions, it may be advisable to pass the beam twice through the volume being investigated, to increase sensitivity

in case of slight variations of the refractory index   (reflection of the
illuminating beam behind the volume being scanned).

The schlieren technique is a mature imaging method of high sensitivity and
highly varied applicability. It is best suited to the attainment of a sur-
vey of density structure in gas flows. Quantitative local determinations,
on the other hand, usually cannot be derived from schlieren images. For this
reason, no further details will be given here and reference is made to /28/.

4.3 Interferometry

Very slight changes in the index of refraction resulting in no recordable
deflection of the beam and thus invisible for the shadow and schlieren me-
thods, may be detected by recording the phase shifts produced by them in the
object waves with respect to stationary reference waves. The basis of the
recording of phase shifts is the interference capability of coherent waves.
The fundamental measuring apparatus for interferometry (the Mach-Zehnder in-   /23/
terferometer) is shown in Figure 16. The coherent, parallel illuminating
beam is divided in an object beam penetrating the volume to be scanned
and a reference beam travelling along a path of approximately equal length
around the volume. Both of the beams are subsequently reproduced together
coaxially on a screen. If both both beams form planat wave fields with iden-
tical positions of the phases, a homogeneous intensity distribution is ob-
tained on the screen. If, on the other hand, the object beam experiences
wave front distortions because of density variations in the object, together
with local phase shifts, interference strips are produced on the screen. If
it is possible to determine the order of the interference strips, i.e. to de-
termine the number of wave lengths by which the phase of the object beam has
been shifted with respect to the reference beam, the wave front of the object

beam when exiting from the object may be determined. The difference in the wave fronts when entering and leaving the object yields the local changes in the optical wave length in the object and thus the variation of the index of refraction integrated over the length of the object. From the variation of the index of refraction the density variation and under suitable conditions the temperature or concentration distribution in the range under investigation may be determined.

In addition to the zero field setting of the interferometer shown, there exists another mode of operation, which produces interference strips if the object beam has not been disturbed (finite fringe method). This reference strip field is attained by a slight defocusing of a mirror in the inferometer. Its deformation with the onset of density variations in the field investigated in general yields a better overview of the proceedings than the method of infinite strip distance (zero field method).

Bright strips are produced when the phase positions of the reference and object beams differ by a multiple of λ; dark strips are generated by multiples of $\lambda/2$. If this multiple is designated by S, then for the bright strips:

$$S \cdot \lambda = \int_{0}^{L} (n - n_0)\, ds$$

It follows from the Gladstone-Dale equation that:

$$S \cdot \lambda = \int_{0}^{L} K\, (\rho - \rho_0)\, ds$$

If the density ρ is constant along L, i.e. a two-dimensional density field is present, then

$$\rho\,(x,y) = \frac{S\,(x,y)\cdot\lambda}{K \cdot L} + \rho_0$$

If the density field $\rho\,(x, y)$ has been produced by a temperature field, /24 then in this simple case

$$T\,(x,y) = \frac{\rho}{R\rho\,(x,y)} = \frac{\rho/R}{\dfrac{S\,(x,y)\cdot\lambda}{K \cdot L} + \rho_0}$$

The interference strips thus represent isotherms. Interferograms are general-
ly evaluated in this manner. If the irradiated objects are rotation symmetric,
the evaluation becomes more complex. In the case of three-dimensional fields
of refractory indices without symmetry properties, interpretation of the in-
terferograms without additional information is not possible.

A series of modifications of the Mach-Zehnder interferometer exists, e.g.:

- the Michelson interformeter (double sensitivity because of passing
twice through the measuring path /29/

- schlieren interferometer (combination of a schlieren apparatus and
a Michelson interferometer /30/

- differential interferometer (both partial beams, produced by means
of a Wollaston prism, are closely adjacent to each other and penetrate the
experimental volume; this yields the gradient of the refractory index in
this partial range /31/

- Hook method (the combination of a Mach-Zehnder interfometer and a
spctrograph with the purpose of deriving from the variation of the index of
refraction recorded information concerning the composition and thermodynamic
state of the gas under investigation /32/

- Holography interferometer (the combination of a Mach-Zehnder inter-
ferometer and the holographic exposure technique).
Instead of presenting further details, reference is made to the relevant
specialized literature. Because of its timeliness, its varied applicability
and relative simplicity, however, the technique of holographic interferometry
will be treated in somewhat more detail.

4.4 Holographic Interferometry

Holographic interferometry combines the interferometric visualization of
gradients of the index of refraction with the technical storage capabilities'

of holography. Let us therefore initially discuss the principle of holography.

4.4.1 Methods of Holography /33, 34/

Holography is a technique of storing optical waves. In a manner similar to the recording of acoustic waves by means of the magnetic tape technique which then may be reproduced stereophonically at will, three-dimensional optical fields of waves may be stored and reproduced. To preserve the full informational content of a field of waves, the amplitude distribution (conventional photography) and the phase position distribution of the wave field must be recorded. The phase position distribution is visualized for the photographic material by superposing a coherent reference beam on the wave field emanating from the object, which by means of interference produces a light-dark distribution that may be photographed by conventional means. The photographic plate in which the interference pattern is stored, is called a hologram. The hologram contains the image of the object exposed in a coded form; the mere viewing of the hologram does not reveal the information. A second step is required to uncode the information: the reconstruction of the object wave field. The field of waves originally emitted by the object is reconstructed and the object itself visualized in the process, by placing the hologram in the path of the reference beam in the same position it occupied during the exposure. The reference beam is refracted by the stored interference pattern in a manner similar to a grating. The first order of refraction is identical with the original field of object waves.

The fact that the amplitudes and phase positions of optical waves are being stored by means of holography, is essential, together with the requirement of using coherent light in the two-step process (e.g. laser light) and that the resolving capability of the photographic plates must be high.

If an irradiated body is exposed, one speaks of incident light holography. The optical apparatus required is shown in <u>Figure 17.</u> The reference beam is obtained by means of beam splitting from the illuminating beam, in order to maintain coherency. The path from the beam splitter to the holographic plate should be approximately equal for the object and the reference beams; the difference in the optival path must be smaller than the coherence length of the source of light.

Transparent media are examined in transmission light. The optical apparatus for transmission holography is quite similar to that of incident light holography <u>(Figure 18)</u>.

The effect useful for measuring purposes of incident and transmission holography becomes apparent only when one proceeds to <u>holographic interferometry</u>. If during the reconstruction of the object wave the object is left standing <u>/26</u> in the illuminating beam, two waves may be observed behind the hologram: the wave emanating directly from the object and the wave reconstructed by the hologram. The two waves are coherent and thus capable of interference. If a slight change is made on the object, e.g. a tiny deformation, the observer will note that the object is covered by the interference strip. The configuration and distance of the interference strip provide information concerning the location and magnitude of the deformation. This technique -- the comparison of two slightly different state of the object -- is designated holographic interferometry.

The following advantages are obtained compared to classical interferometry: because both of the wave fields required for interferometry emanate from the object, only changes made on the object itself are visualized. Changes in the field of waves due to defective optical parts, boundary layers at

windows, etc. are immaterial, because they are superposed on both fields of waves similarly. Holographic interferometry is possible even when the object is covered by a matte plate. In contrast, in classical interferometry, the highest optical quality of the apparatus and absolute freedom of interference of the wave field outside the object range must be observed, Further, optical parts may be kept relatively small in holography, because divergent light may be used without harmful consequences. This favors the use of mechanically stable arrangement which is essential for the investigation of nonstationary processes.

Holographic interferometry makes it possible to store both object wave fields to be used in interference. This technique is called double exposure holography. Through the use of double pulse lasers the exposure intervals may be kept extremely short so that rapidly changing processes may be analyzed. Because of the high sensitivity of holographic plates therefore significantly more rapid image sequences are obtained than with classical interferometers and conventional exposure techniques.

The storing of object waves renders their reconstruction possible over periods of time of arbitrary length. Instantaneous exposure may thus be examined subsequently by means of a great variety of methods. For example, the field of waves may be scanned in depth, which is not possible with conventional photographic methods.
If variable processes are observed by the so-called real time method, i.e. when the instantaneous situation is continuously compared with the stored reference situation (zero hologram), another advantage compared with conventional interferometry is gained: the reference state is absolutely stable, it is not necessary to keep the reference beam constant as in conventional

interferometry.

The possibilities of conventional interferometry are thus made accessible by
the introduction of holography and are expanded with respect to precision.

4.4.2 Application of Holographic Inferometry in Incident Light

Let us cite the investigation of plastics particles as an example for real
time holography. The apparatus necessary for the deformation investigation of
of a wound plastic tube with a nominal width of 300 mm is shown in Fig. 19.

Assuming a direction of deformation, the following is generally valid for
the determination of the displacement vector of of a surface element

$$\delta = Z \frac{\lambda}{2 \cos \alpha} \qquad \qquad (E)$$

where δ = radial deformation

z = strip arrangement (number of existing interference
strip counted from the zero stress)

λ = wave length of the laser light used

α = angle between the direction of illumination and ob-
servation.

Figure 20 describes the state of deformation of the inside of the tube in
case of a given differential stress by means of internal pressure.
Investigations of this type, as performed at the present time at DFVLR, are
necessary for the support of development work, in failure analysis and the
local quantitative determination of deformations and stress fields. Deforma-
tions of the order of magnitude of 1 to 100 μm may be recorded.

4.4.3 Application of Holographic Interferometry in Transmission Light

One problem is common to all of the measuring methods which visualize va-
riations of the index of refraction. It is generally not possible to decide
whether the changes in the index are the result of temperature or concentra-

tion gradients. The question may be answered unamiguously in a few cases only. In evaporation, ablation, combustion and similar processes the exchange of heat and material are always coupled to each other, so that the following equation describes the variation of the length of the optical path:

$$S\lambda = 1\left[\left(\frac{\partial n}{\partial T}\right)_C \cdot \Delta T + \left(\frac{\partial n}{\partial C}\right)_T \cdot \Delta C\right] \tag{F}$$

where

S = a multiple of the wave length

1 = length of the experimental volume

n = index of refraction

T = temperature

C = concentration

The index of refraction depends not only on temperature and concentration, but also of the wave length of the incident light. This means that different interference patterns are produced for different wave lengths. If, for example, a binary material system is irradiated by two wave lengths and the two interference fields recorded simultaneously, the temperature and concentration distribution may be determined by evaluating the interference pattern. With multicomponent systems the number of interference patterns required must be increased in keeping with the number of components. Because the dependence of the index of refraction on the wave length is very small, up to the present time, success was achieved with holographic two wave lengths interferometry only. As an example, let us cite the work of Panknin /35/ in determining the heat and material transport in a flat plate; this may be determined very accurately by this method.

The measuring apparatus is shown in **Figure 21.** The open arrangement corresponds to the layout outlined above for transmission holography with the

exception of the second laser beam reflected in with the same optical axis. Both laser beams pass through the shutter V so that the synchronous recording of both interference pattersn is assured.

The performance of an interferometric measurement with two wave lengths is outlined in Figure 22. The double exposure hologram is prepared by means of the simultaneous exposure of the comparision state and the measuring state with both wave length and subsequently reconstructed and photographed, by activating the two reference beams successively. The strip positions of the two inferograms are measured accurately with a microscope and converted into a temperature profile and a concentration profile. To reduce the problems of coordination which are always associated with the use of two images, it is convenient to arrange the holographic plate in the plane of the film; this eliminates the preparation of film images and assures the secure spatial coordination of the two interference patterns.

The interferograms of the superposed temperature and concentration boundary layer with free convection of a vertical plate is shown in Figure 23. In order to produce the temperature boundary layer, the plate was heated uniformly, the concentration boundary layer was obtained by evaporating and thinly applied layer of naphthalin. Finally, the evaluation of these inferograms is shown by the result presented in Figure 24. These curves may be determined for sections at any height. If the naphthalin layer is replaced by a fuel film, difficulties arise in interpretation; these are primarily the result of the very high line densities in the vicinity of the wall and the very weak dependence of the indices of refraction on wave length. The application of two wave length interferometry in combustion processes to determine the temperature distribution and the unburned portion of the fuel is limited at the present time; the limits can probably be overcome by the use

of lasers with greater frequency intervals.

4.5 Laser Anemometry

Laser Doppler anemometry is used to determine the velocity of particles suspended in flowing media or added to such media. By superposing two coherent laser beams a local bright-dark field is generated (interference pattern), which becomes visible during the passage of the particles. The light scattered by the particles (Mie scattering) is sufficient to be recorded by sensitive photodetectors. An alternating voltage is generated at the detector outlet, the frequency of which represents a measure of the particle velocity in a defined direction. The fundamental design for such particle velocity measurements is shown in Figure 25.

The formal relationship between velocity and frequency is as follows:

$$\nu = \frac{2\,n\,V_\perp}{\lambda_0}\,\sin\frac{\alpha}{2}. \tag{G}$$

where

ν = frequency of the alternating current

n = index of refraction

V = velocity of scattering particles perpendicular to the center line of the angle of the laser beams

λ_0 = wave length of radiation, with respect to vacuum

α = angle between the laser beams

This frequency is identical with the beat frequency which results from viewing the optical signal recorded as the superposition of two Doppler signals displaced in frequency with respect to each other, the signals being produced by the two Laser beams and the moving particle. This interpretation gave the method its name.

The particle size required may be critical, because minimum diameters are ne-
cessary for reasons of the recording technology (> 0.1 µm). The resulting
behavior of these particles, which are large compared to molecular dimensions,
is considered not generally satisfactory especially in nonstationary processes.
In stationary flows without excessive velocity gradients it may be assumed,
however, that the particle velocity measured is identical with the flow velocity.

One-, and two-dimensional Doppler anemometry with determination of the direction of
the selected velocity components can be done relatively easily today using commer-
cial equipment. There are still problems measuring the third velocity component,
especially problems associated with reducing complexity. However, in principle
there is a solution here as well. In order to be able to measure very closely
to the surrounding walls, to improve the signal-to-noise ratio, experiments were
performed. This involved separating the optical frequency range of the measured
signal and the incoming light frequency by exploiting fluorescence phenomena.
The references [10, 29, 36] give a good summary of the state of the art of laser-
Doppler anemometry.

The two-focus method [37] is an interesting modification of the two-beam Doppler
method, which is shown in figure 26. Compared with the Doppler method, the strip
system is eliminated, that is, the two laser beams are no longer focused onto a
common point, and both beams are focused separately. The diameters of the generated
lighting limits can be made very small. Their separation can be varied almost at
will. Since a minimum number of fringes are required in the Doppler method, in
order to guarentee an exceptable accuracy of frequency measurement, the intensity
of the laser beams is distributed over a relatively large area. On the other hand,
in the two-focused method, the focused points can be extremely small, and therefore
the intensities can be extremely large. Consequently, one can operate with substantially

smaller scattered particles using this method. In addition, the frequency measurement is replaced by a much simplier measurement of the flight time from one barrier to the next.

4.6 Particle Field Holography

It is of great interest to develop a measurement method which can make visible the size and velocity distributions of particles imbedded in floes, which will allow the obtaining of information regarding the particles. The Mie scattering effect already allows one to determine certain information about the particles. The scattering with small particles is another effect which allows a recording and analysis of particle fields in conjunction with holographic methods.

If parallel and monochromatic light impinges on a particle whose diameter is not very different from the wavelength of the light, then a light-to-dark distribution will be of observed behind the particle which is called the refraction figure. The refraction figure appears as concentric circles for round particles. It is due to the superposition of elementary waves which emerge from each point of the particle contour. Due to their coherence, they will interfer.

If a photographic plate is placed in the path of the beam, a hologram is generated by the superposition of the refracted pattern which is considered the object beam and the light passing the particle without ingerference, this light acting as the reference beam. The reconstruciton of the hologram yields the refracted pattern. Be means of a laser pulse, the diffraction image of all of the particles moving within the experimental volume may be sotred as an instantaneous image. A second exposure with a predetermined time interval makes it possible to determine displacements and particle velocities.

38

One possibility of the evaluation of the holograms consists of measuring the ring

structures with a microdensitometer directly on the holographic plate

and convert them by means of the theory of diffraction into particle diameters

and distances immediately from the plate. Because two values are to be '

determined per particle (diameter and distance), tow items of measured infor-

mation must be taken from the hologram. These consist of the distance of the

diffraction rings and the intensity of the bright fields. The preparation of the

microdensitometer curves of a multitude of diffraction patterns and the computing

effort required render this method less than attractive. A simplier method of

evaluation is shown in Figure-27   from /38/. During the reconstruction of

the hologram by means of a continuous wave laser a real image of the experimental

volume is generated in the position outlined; this

may be visualized on a matte plate. To obtain a magnification of the object represented on a 1:1 scale, small areas of the matte plate are reproduced on a Vidicon tube , which in turn produces an enlarged image on a monitor. By displacing the hologram parallel to the axis of the beam, any plane of the volume investigated may be reporduced on the monitor. The bright center of the diffraction pattern is focused sharply and the evaluation performed. With the particle velocities, e.g. in flames, even very short exposure times may cause loss of sharpness and thus evaluation problems. This limits the method.

4.7 Visualization by means of Electronic Stimulation

If because of slight densities the changes in the index of refraction are so small that they cannot be visualized with the schlieren method or inferometry, other methods must be used. An alternative solution is offered by gaseous discharge in which molecules are electronically excited in the range of discharge, thus causing them to emit light. The intensity of the optical phenomenon is a measure of density.

Direct, alternating and high frequency sources are used in gas discharge. Direct current gas discharge may be affected generally with densities amounting to approximately 10^{-1} of standard density. An ignition voltage is, however, required; this voltage must be considerably above the operating voltage (about 1000 V) in order to produce adequate conductivity in the area under investigation. Depending on the shape and polarity of the electrodes, a more or less homogeneous intensity distribution is developed in the intermediate area. Increased homogeneity of the optical phenomenon may be achieved by applying an alternating voltage. The light density and propagation the gas discharge depend substantially on the distribution of field strength on the volume of gas and to what extent the density of the gas permits ionic diffusion. In direct and alternating voltage gas discharges the field

40

strength are largely a function of electrode configuration. To avoid this limitation , it is advisable to use high frequency alternating fields to produce high field strengths in larger volumes. The problem here consists of a suitable arrangement to transfer the high frequency energy to the gas. Solutions are described in /30/; the brightness values attained are sufficient to produce color images.

Electron beam fluorescence has already been discussed in detail as a spectroscopic method. The visible trace left by the electron beam in the area investigated, in addition to local state analysis, may also be used to visualize a flow field. Through the periodic deflection of the electron beam, an illuminating spectrum is created, which visualizes the planes of the flow field. The image brightness is sufficient to permit the application of various quantitative evaluating methods (densitometry, equidensity methods, photomultiplier recording) and to determined density profiles.

5. Conclusions

In spite of the great progress achived in recent years in the field of optical measuring technology, it should be noted that the determination of three dimensional flow fields and nonstationary processes still has its problems. Imaging methods in general yield integral results and make it difficult to distinguish between temperature and concentration effects; light scattering methods provide local information, but are weak in the area of time resolution of nonstationary processes, because relatively low capacity continuous wave lasers require long integration times (photon counting), while pulse lasers do not permit sufficiently high repeating frequencies. In the present state of development therefore, the following methods should /33 be further developed with high priority:

- development of Raman spectroscopy on an impulse laser basis with the objective of performing local measurements in time resolution,

- development of transmission light holography on a pulse laser basis to perform global, three-dimensional measurements in time resolution,

- a combination of the two methods, in which Raman spectroscopy provides the reference state for holographic interferometry.
The authors hope that they were able to provide stimuli for additional work and the solution of problems in thermogasdynamics.

6. References:

/1/   Griem, H.R.   "Plasma Spectroscopy" New York, McGraw-Hill, 1964

/2/   Lochte-Holtgreven   "Plasma Diagnistics" Amsterdam, 1968, North-Holland Publishing Co.

/3/   Twardy, H. & H. Selzer "The Use of the Line reversal Method in Temperature Measurements in the Combustion Chamber of a Rocket Engine" DLR FB 70-70 (1970)

/4/   Gaydon, A.G.   "The Spectroscopy of Flames" New York, Wiley, 1974

/5/   Erhardt, K. & Schweiger, G.   "Influence of electron beam-body interactions on vibrational temperature measurements" Progress in Astronautics and Aeronautics, Vol. 51, II (Potter, Jl.L., ed. pp. 1305-1312, 1977)

/6/   Schweiger, G.   "Experimental investigation of local density and temperature distribution in a flow field around a spherical model with a strong thermodynamic nonequilibrium by the electron beam method" DLR FB 77-29 (1977)

/7/   Schweiger, G Becker, M.   "Investigation of Shock-Shock Interaction in Hypersonic Flow: Rarified Gas Dynamics, Progress in Astronautics and Aeronatutics, Vol. 51, I (J.L. Potter,ed). pp. 435-445.

/8/ Schweiger, G Papanikas, D.G. Fiebing, M.   "Temperature Measurements in the Flow Field Around Simple Bodies in a Hypersonic, High-Enthalpy Flow" Int. Congress on Instrumentation in Aerospace Simulation Facilities. ICIASF '75 CHO 993-6 AES, pp. 229-236

/9/ Graham, S.C. & al. "Transient Molecular Concentration Measurements in Turbulent Flow Using Rayleigh Light Scattering AIAA Journal, Vol. 12, No. 8 (1974) pp. 1140-1142

/10/ Goulard, R. "Combustion Measurements. Modern Techniques and Instrumentation", New York, 1976, Academic Press

/11/ Self, S.A.
Kruger, C.H. "Diagnostic Methods in Combustion MHD Flows" AIAA Paper No. 76-310 (July, 1976)

/12/ Setchell, R.E. "Time Averaged Measurements in Turbulent Flames Using Raman Spectroscopy"' AIAA Paper No. 76-28 (January 1976)

/13/ Lapp, M.
Hartley, D.L. "Raman Scattering Studies of Combustion" General Electric Report No. 75 CRD 195 (October, 1975)

/14/ Lapp, M. "Optical Diagnostics of Combustion Processes" SPIE, Vol. 61, 42-50 (1975)

/14/ Lapp, M. "Flame Temperatures from Vibrational Raman Scattering" General Electric Report No. 74 CRD 062 (March, 1974)

/16/ Lederman, S. Modern Diagnostics of Combustion AIAA Paper No. 76-26 (Januray 1976)

/17/ Lederman, S. "Some Applications of Laser Diagnostics to Fluid Dynamics" AIAA Paper No. 76-21 (January, 1976)

/18/ Salzman, J.A. & al. "Determination of Gas Temperatures from Laser-Raman Scattering" NASA TN D - 6326 (May 1971)

/19/   Williams, W.D.   "Rotational Temperature and Number Density Mea-
Lewis, J.W.L.

surements of N_2, O_2, CO and CO_2 in a Hypersonic

Flow Field Using Laser Raman Spectroscopy

AEDC-TR-75-37 (July 1975)

/20/   Williams, W.D   "Hypersonic Flow Field Measurements Using Laser-   /36

Lewis, J.W.L.   Raman Spectroscopy"

AIAA J. 13(10), 1269-1270 (October 1975)

/21/   Regnier, P.R. & al.   "Gas Concentration Measurement by Coherent Raman

Anti-Stokes Scattering'
AIAA Paper No. 73-702 (July 1973)
AIAA Journal 12(6) June, 1974, 826-831

/22/ Moya, F. & al.   "Gas Spectroscopy and Temperature Measurements

by Coherent Raman Anti-Stokes Scattering"

Optics Communications 13(2) (February 1975)

169-174

/23/   Moya, F. & al.   "Flame Investigation By Coherent Anti-Stokes

Raman Scattering"

AIAA Paper No. 76-29 (January 1976)

/24/   Hirth, A.   "CW Coherent Anti-Stokes Raman Scattering from
Vollrath, K.

Gases"

ISL-CO 216/76 (June 1976)

/25/   Roh, W.B.& al.   "Single Pulse Coherent Anti-Stokes Raman Scattering"

Applied Physics Letters, 29(3) (August 1976)

174-176

/26/   Mie, G.   "Contribution to the Optics of Turbid Media

Particularly Collodial Metal Solutions"

Ann. Phys. 25 (1908), 377-447

/27/   Katerle, H.J.   "Measurements of the Back Scattering on Mole-

cules and Aerosols in the Stratosphere   by means

of Ruby Laser Beams from the Ground"

Dissertation, Munich University, 1969

/28/   Wuest, W.   "Flow Measuring Technology"

uni-text, Braunschweig, Vieweg &Son, 1969

/29/ Trolinger, J.D.   "Laser Instrumentation for Flow Field Diagnostics"   /37/

AGARD-AG-186 (March 1974)

/30/   Deutsche Gesellschaft   Report on the 4th Meeting of the DGLR Specialist
        fur Lufy & Raumfahrt

Committee "Flow Mechanics Research", October

23/25 1972, Friedrichshafen

"Optical Methods of Flow Measuring Technology"

Part I, DLR Mitt. 73-20 (1973)

/31/   Smeets, G.   "Experimental Determination of the Thermal Conduc-

tivity   of Air and Air/Water Vapor Mixtures in

the Temperature Range of 2000 $\leq T \leq$ 7000°K"

ISL Report R 118/75 (May 1975)

/32/   Dosanjh, D.S.   "Modern Optical Methods in Gas Dynamics Research"

New York, Plenum Press, 1971

/33/   Kienle, H.   "Introduction in the Technology of Holography"
        Ross, D.

Frankfurt/M. Akad. Verlagsgesellschaft, 1969

/34/   Pankhurst, R.C.   "Laser Technology in Aerodynamic Measurements"

AGARD-LS-49 (March 1972)

/35/   Panknin, K.   "A Holographic Two-Wave Length Interferometry

to Measure Superposed Temperature and Concentration

Boundary Layers"

Dissertation, Hannover Technical University, 1977

/36/   AGARD   "Applications of Non-Intrusive Instrumentation in Fluid Flow Research" AGARD-CP-193 (September 1976)

/37/ DGLR   Report on the 4th Meeting of the DGLR Specialist Committee "Flow Mechanics Research" 23/25 October 1972, Friedrichshafen "Optical Methods of Flow Measuring Technology" Part 2, DRL Mitt. 73-21 (1973)

/38/   Gabler, H.D.   "Application of Pulse Holography to the Investigation of Moving Particle Fields" DLR-Mitt. 73-34 (1973)
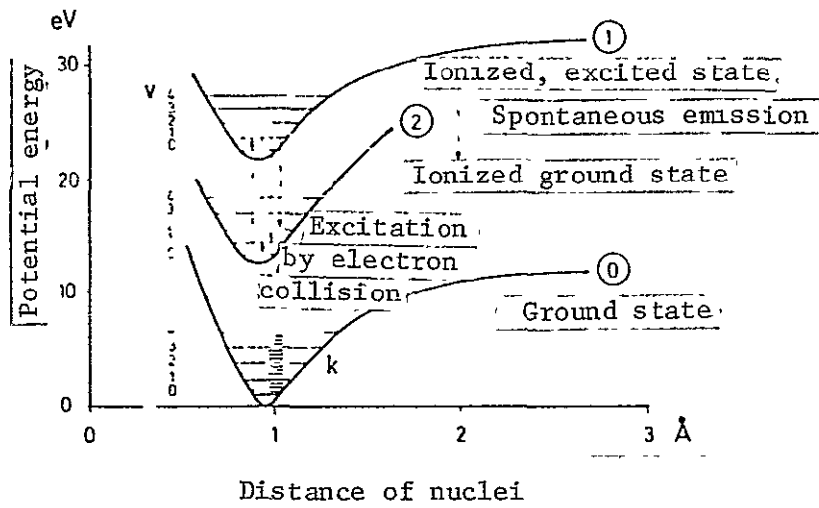
Figure 1. Principle of electron beam fluorescence
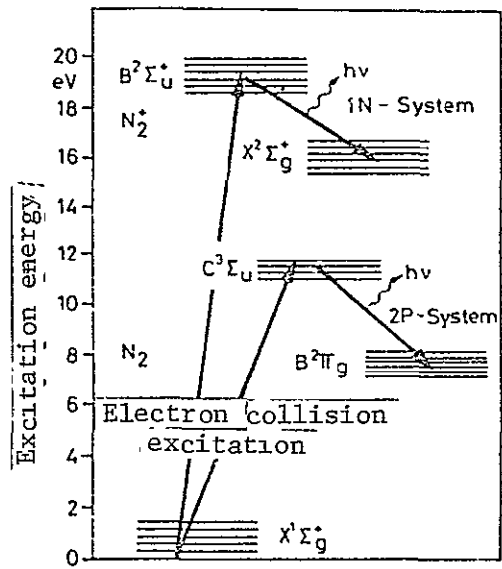
Figure 2. Excitation mechanism of the
1 N and 2 P system of nitrogen by
electron impact
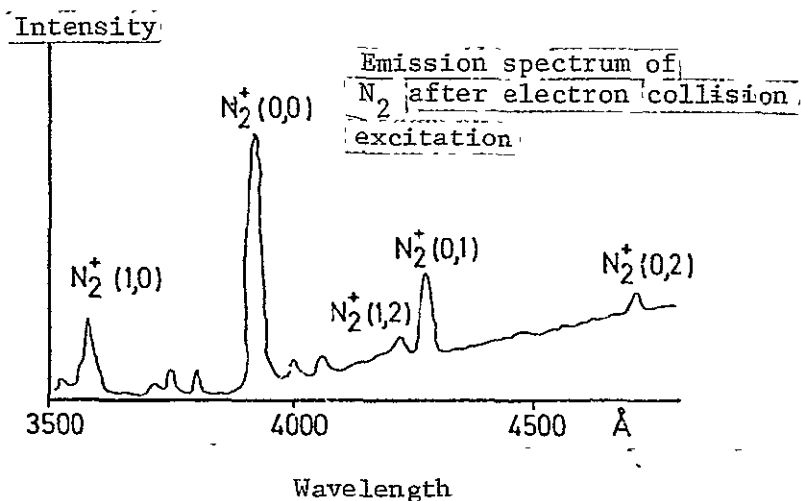
Figure 3. Electron beam induced nitrogen fluorescence
with the bands of the first negative system
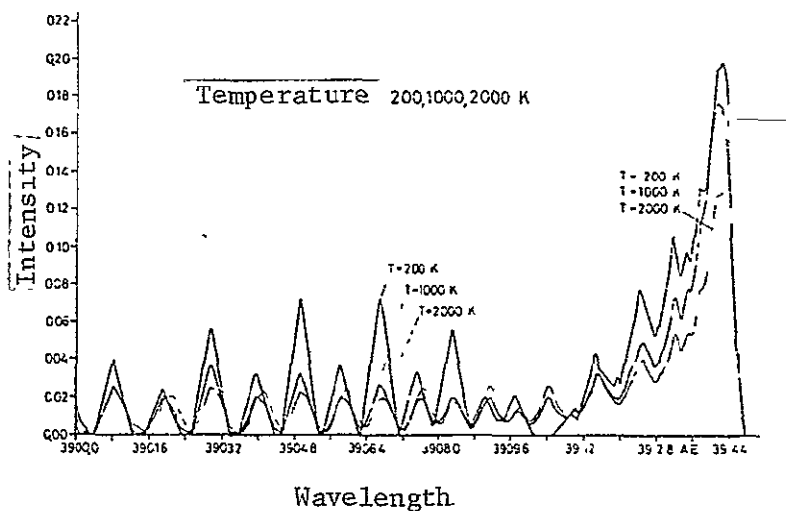
Figure 4. Synthetic spectra at different rotational temperatures
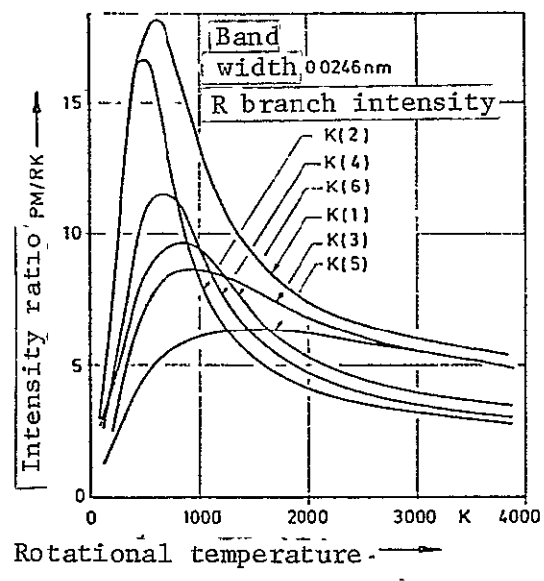
Figure 5. Relationship of the maximum
intensity in the P branch to the first
five intensity maxima in the R branch
as a function of gas temperature
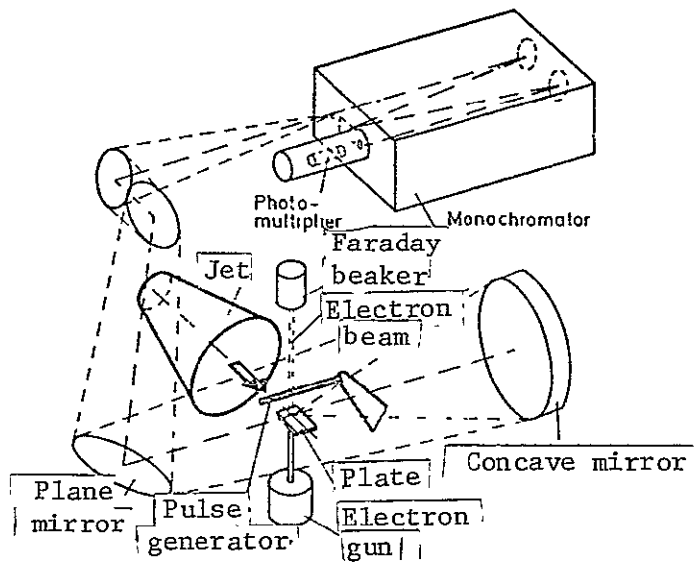
Figure 6. Experimental setup to determine
the electron beam fluorescence in the gage
length of a wind tunnel
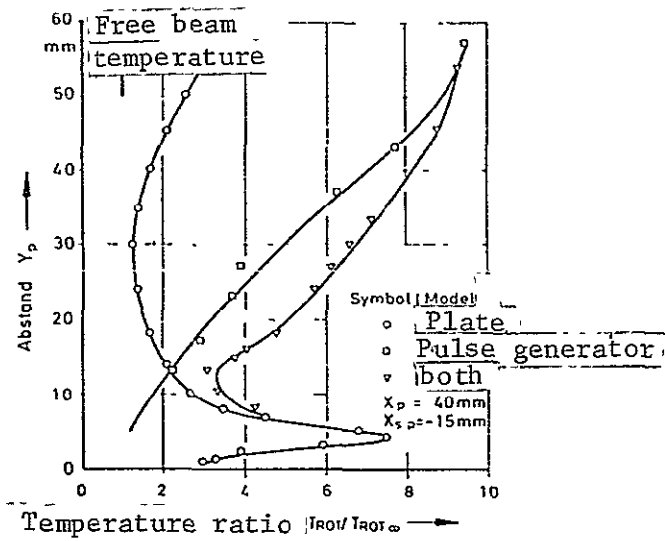
Figure 7. Profiles of the rotation temperature on the plate and pulse generator independently of each other and in interaction
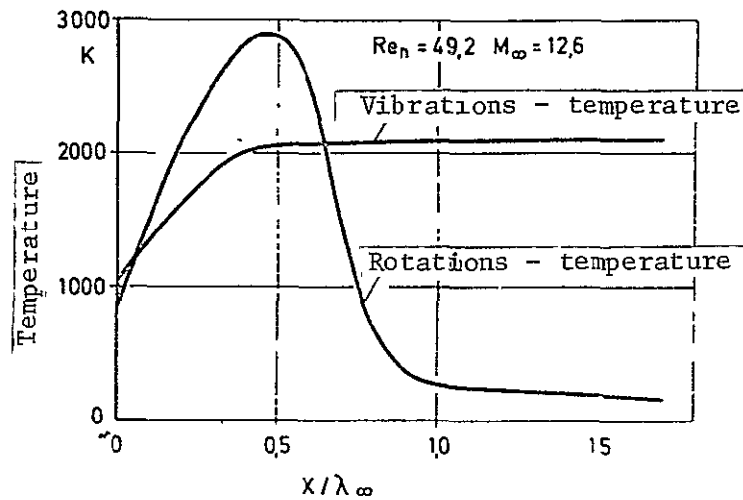
Figure 8. Temperature distribution in a non-equilibrium flow in front of a spherical model

51
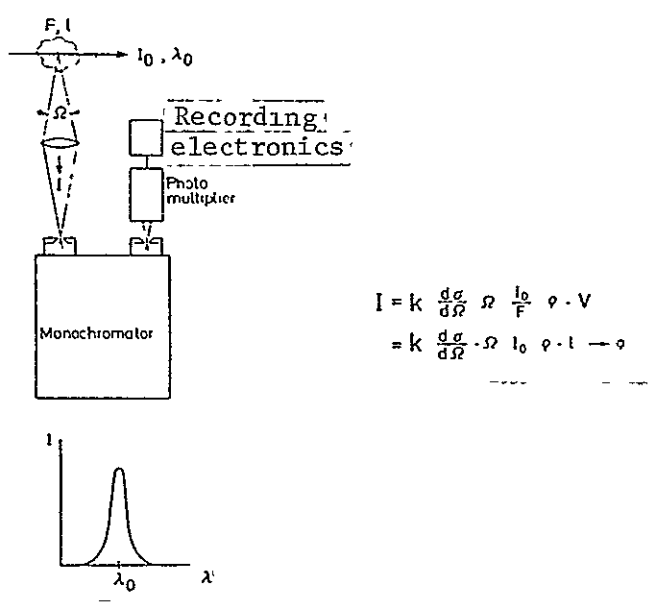
$$I = k \frac{d\sigma}{d\Omega} \ \Omega \ \frac{I_0}{F} \ \rho \cdot V$$

$$= k \frac{d\sigma}{d\Omega} \cdot \Omega \ I_0 \ \rho \cdot l \longrightarrow \rho$$

Figure 9. Principle of Rayleigh scattering measurements

I = Scattered light intensity (number of photons)

k = Constant for the optical efficiency of the setup

$\frac{d\sigma}{d\Omega}$ = Differential scattering cross section

Ω = Opening angle of the recording optical device

I_0 = Laser light intensity (photon number)

= Particle density

L = Length of experimental volume

$V = F \cdot L$; f(split width).

Energy level diagram and Raman line excitation

$$\Delta v = v_0 - v_R = \frac{E_1 - E_0}{h}$$
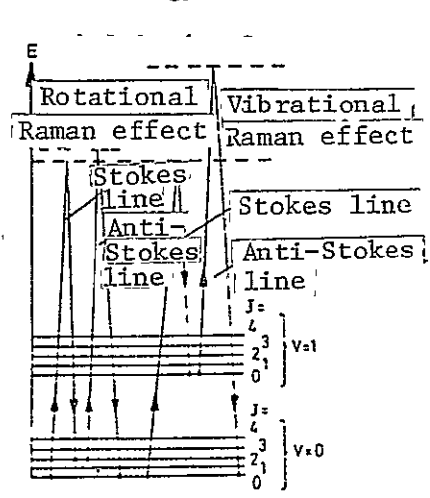
Δv = Raman shift

v_0 = Frequency of incident light

v_R = Raman line frequency

E_1 = Molecule energy (before interaction)

E_0 = Molecule energy (after interaction)

h = Planck constant

$\Delta J = 0, \pm 2$

$\Delta v = 0, \pm 1$

Figure 10. Quantum mechanical explanation of the Raman effect

52
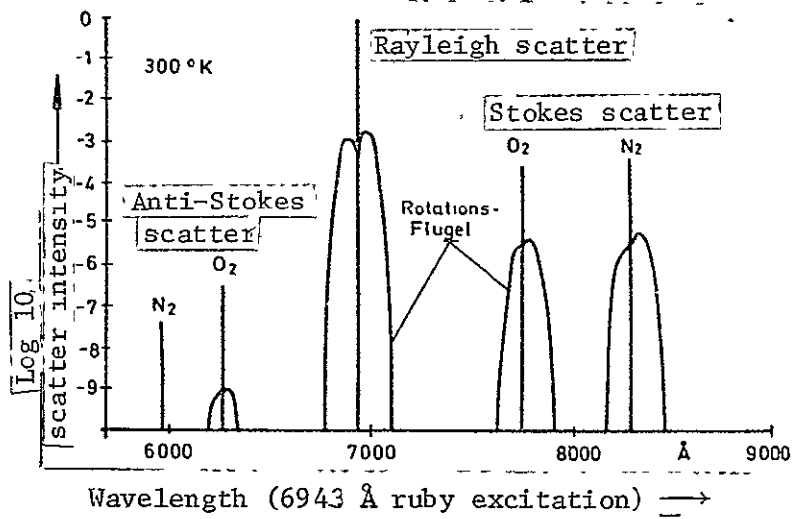
Figure 11. Scatter intensity distribution
for T = 300°K
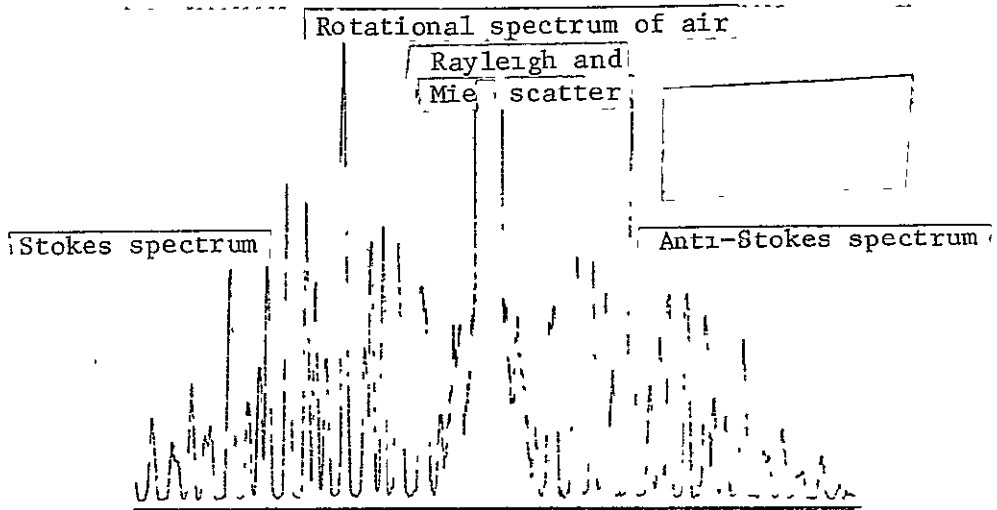
Figure 12. Rotational Raman spectrum of air

λ_0 = 5145 Å Excitation wavelength

Split = 100 μm
Laser capacity = 0.75 w
Tagging - 1 WN
T_0 = 290 K

N₂ rotational spectrum

Excitation wavelength
$\lambda_0 = 5145$ Å
Split = 100 µm
Laser capacity = 0.72 W

Rayleigh and Mie scattering

Marker = 1 WN
$T_0 = 290$ K

Stokes spectrum

Anti-Stokes spectrum
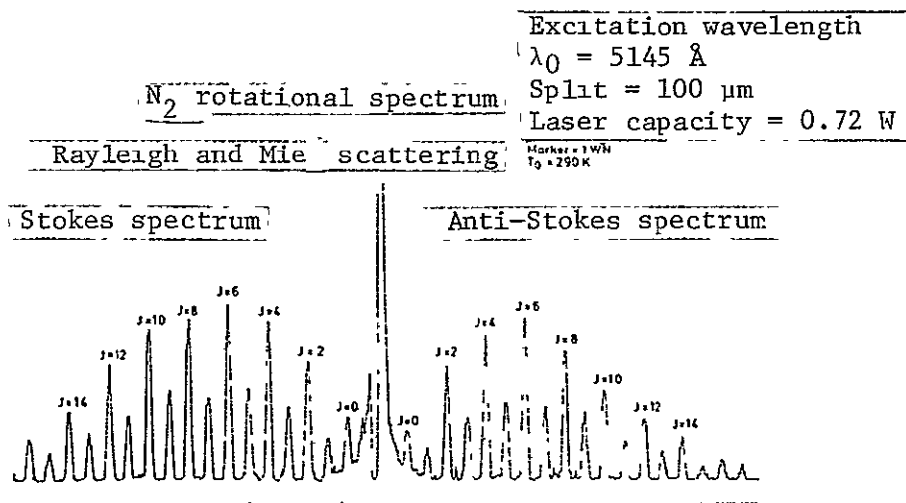
Figure 13. Rotational Raman spectrum of Nitrogen
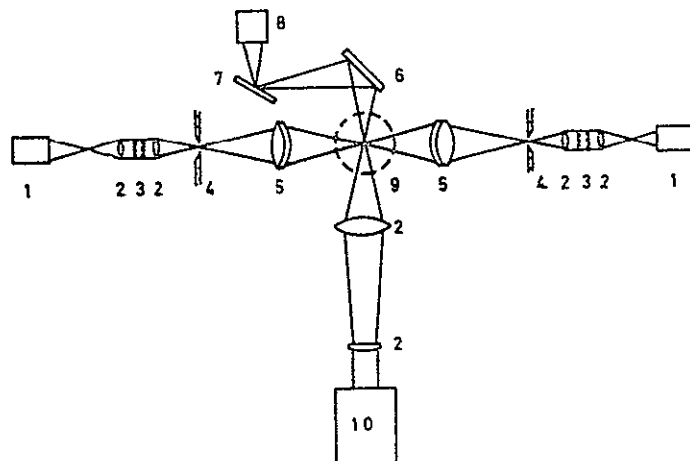
Figure 14. Measuring setup for temperature
measurements using the Raman method

1 Photomultiplier
2 Lens
3 Interference filter
4 Slit
5 Achromat
6 Mirror
7 MGO reflector
8 Calorimeter
9 Experimental
10 Laser head

54
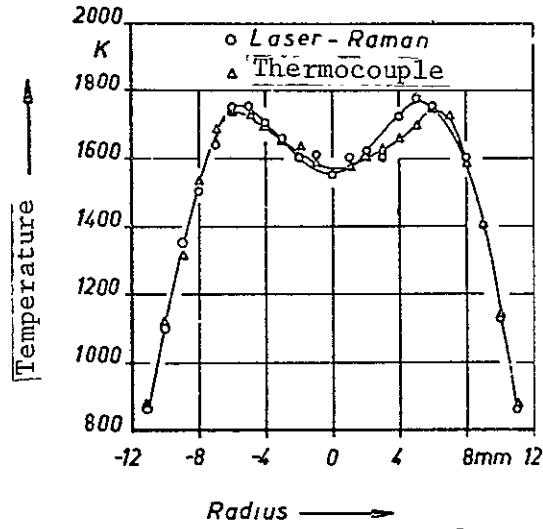
Figure 15.   Temperature distribution in a flame
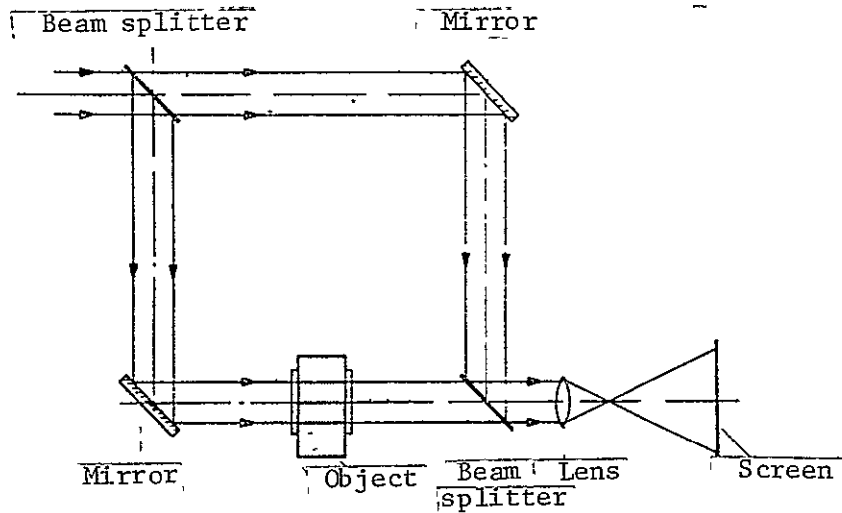
Figure 16.   Conventional Mach-Zehnder interferometer

55
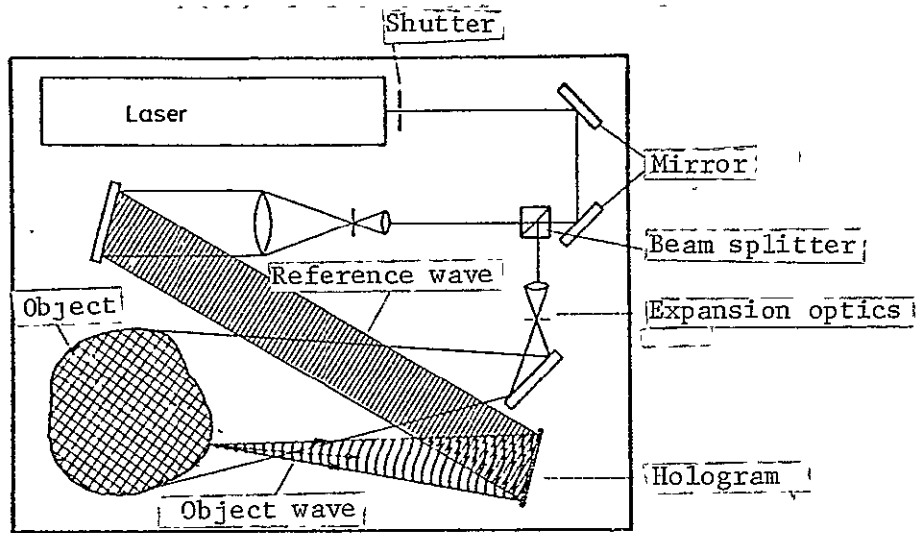
Figure 17. Arrangement for incident light holography
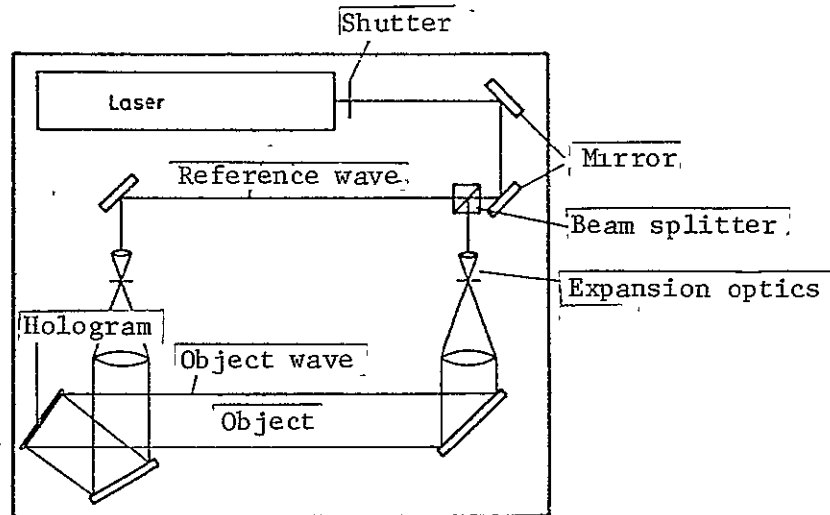
Figure 18. Arrangement for transmission holography

/47
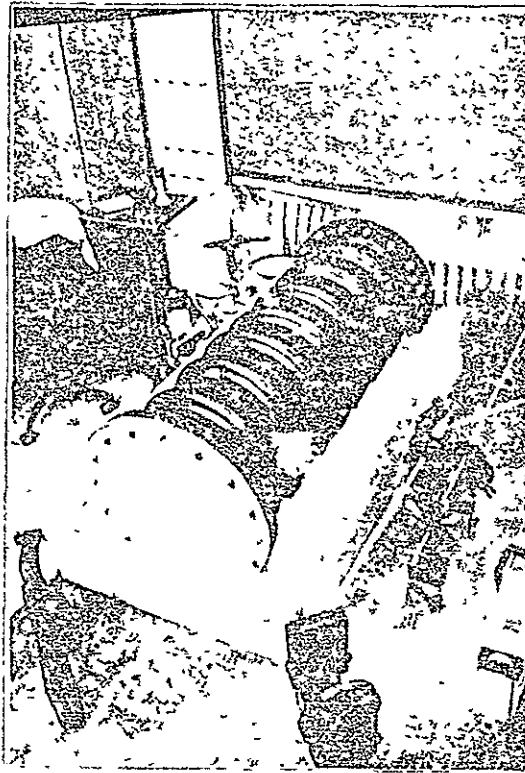
Figure 19. Setup of laser (right), optics, hologram plate
(lower left), pump and pressure measuring instrument (upper
left) and object to be examined

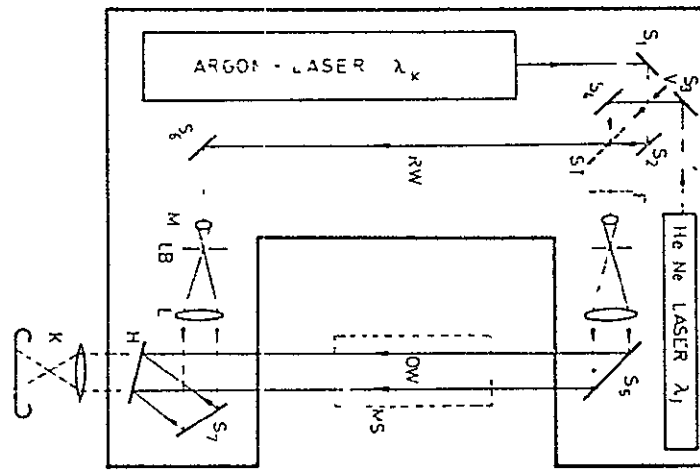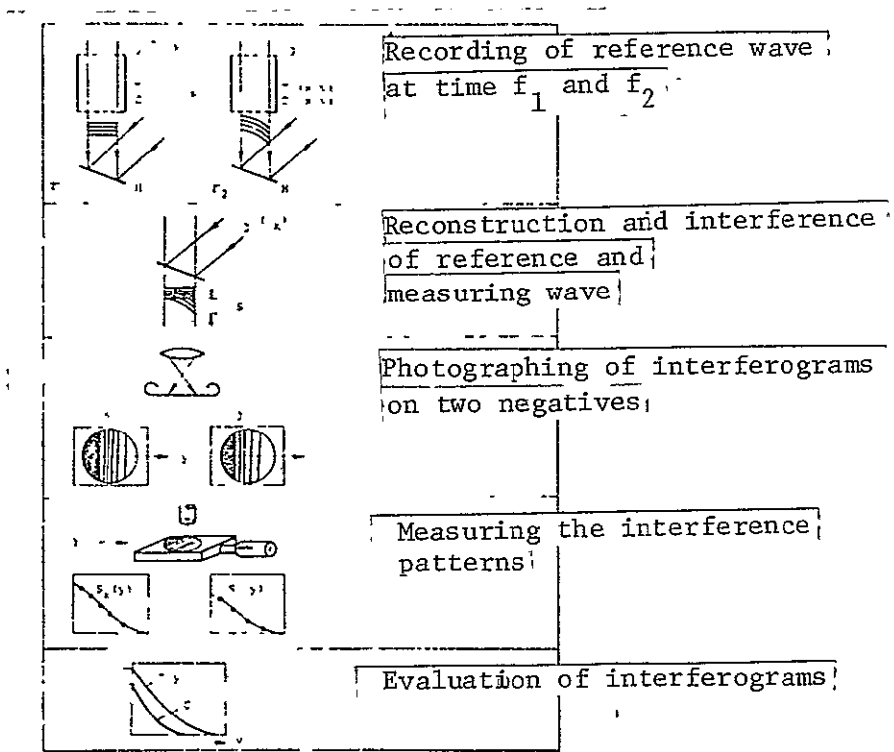Figure 21. Beam path of holographic two-wave
length interferometer
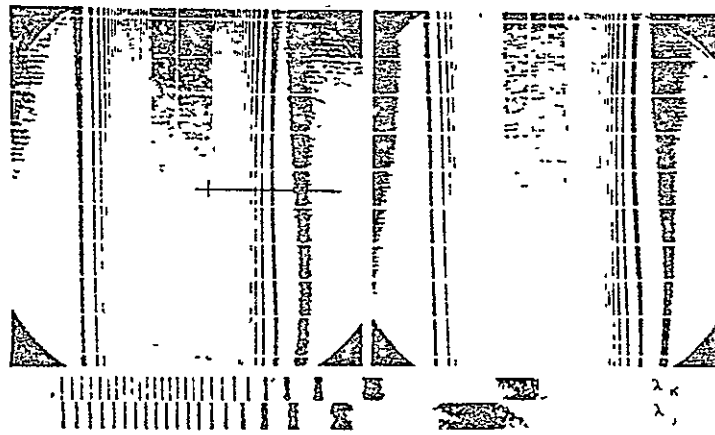

Figure 22. Experimental procedure (schematically)

Figure 23. Interferograms λ_j (left) and λ_k of the superposed temperature and concentration boundary layers on the vertical plate with enlargements of excerpts
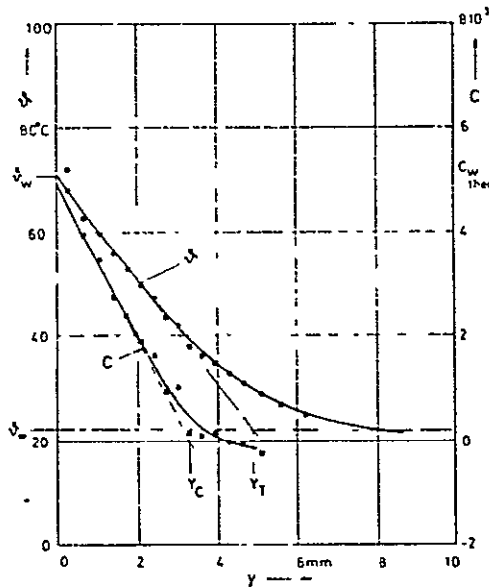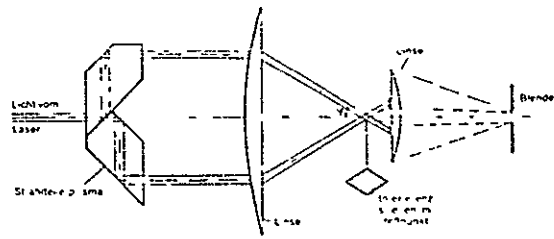

Figure 24. Temperature and concentration profiles as functions of the distance from a plate surface
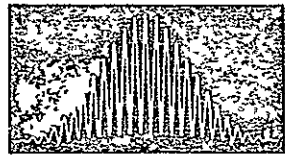
59

ORIGINAL PAGE IS
OF POOR QUALITY

Figure 25. Single channel laser Doppler Anemometer*
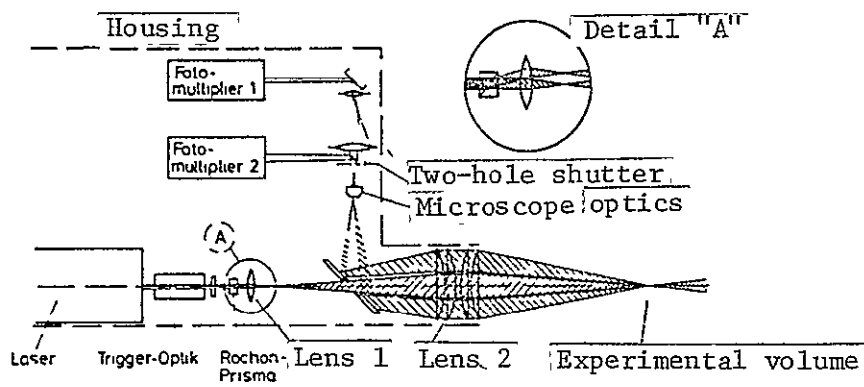*Translator's note. Words in figure illegible.

Housing   Detail "A"

Foto-
multiplier 1

Foto-
multiplier 2
                    Two-hole shutter
                    Microscope optics

(A)

Laser   Trigger-Optik Rochon- Lens 1 Lens 2 Experimental volume
                       Prisma

Figure 26. Two focus laser anemometer by Schodl

Adjusting and
reconstruction laser (He-Ne)

                        Hologramm   evtl Streu-
                                     schirm   Camera   Monitor

Ruby laser
           Nonfocusing Particle eelles   Imaging
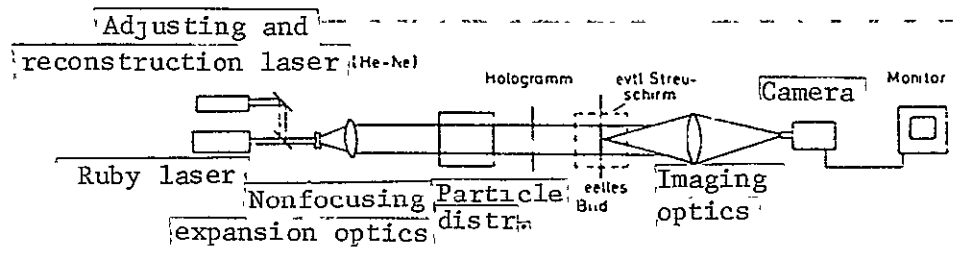   expansion optics distr.   Bild   optics

Figure 27. Setup for exposure, reconstruction,
and evaluation of dynamic particle distribution